

Modelling and Designing Wire-Grid Sparse Antennas Using MoM-based Approaches for Enhanced Performance and Reduced Cost

Adnan F. Alhaj Hasan, Manh Tuan Nguyen, Talgat R. Gazizov

Abstract – In today's competitive market, it is crucial to continually improve antenna manufacturing technologies to keep up with the increasing demands. Researchers can utilize numerical methods to create novel and highly effective antenna designs, pushing the boundaries of antenna engineering. This paper considers two approaches to efficiently model and design sparse wire-grid antennas. The main idea is to create an optimal wire structure that closely approximates the current paths in the antenna while maintaining its integrity with minimal mass. This structure can be used in further simulations with controlled characteristic accuracy and less resources. In this study, these approaches were applied to modelling horn, conical horn, and reflector antennas. The verification was conducted by comparing their results with those obtained from numerical and experimental tests for the same antenna designs. The findings demonstrated good agreement between the results. In addition, we investigated the impact of using these approaches on the antenna characteristics and found that they can enhance the performance of certain characteristics while reducing costs in manufacturing and modelling.

Keywords – Horn Antenna, Conical Horn Antenna, Reflector Antenna, Sparse Antennas, Method of Moments, Optimal Current Grid Approximation, Wire-Grid.

I. INTRODUCTION

Many studies have been conducted on antenna modelling and manufacturing, as antennas are an essential component of any radio electronic device [1]. Thanks to advancements in computational methods, researchers have proposed a wide range of innovative solutions for antenna modelling, particularly, for smart [2, 3], wearable [4, 5], and satellite antennas [6, 7]. These solutions have helped achieve the desirable final product that the market demands. As a result, modern antennas feature small size and lightweight designs, suggest minimal modelling and manufacturing costs, and provide the required characteristics [8].

The advantages of numerical methods can be utilized in the early stages of antenna design process to minimize modelling costs and optimize the antenna structure and characteristics. Additionally, these methods serve as the foundation for new approaches to antenna modelling, resulting in innovative antenna structures with improved performance.

Article history: Received August 12, 2023; Accepted October 30, 2023

Adnan F. Alhaj Hasan, Manh Tuan Nguyen, Talgat R. Gazizov are with the Faculty of Radio Engineering, Tomsk State University of Control Systems and Radioelectronics, 40, prospect Lenina, 634050, Tomsk, Russia, E-mail: alhaj.hasan.adnan@tu.tusur.ru,

However, choosing the appropriate method is not a simple task, as it can significantly impact the total design cost. In the meantime, the method of moments (MoM) [9] can help to eliminate this challenge. This is because MoM is simple and allows for deriving new approaches based on it [10]. Moreover, it has low discretization cost and can provide acceptable results using fewer resources than other methods [11].

The wire-grid (WG) modelling approach is one of the remarkable MoM-based approaches. This approach is popular for its ability to reduce computational costs by approximating the antenna surface with a grid of connected wires in which surface currents flow [8]. A considerable number of studies have been conducted on antenna modelling, especially those related to WG modelling approach [12, 13], since it can significantly reduce the computational cost. It is worth noting that investigations on sparse antennas (SA) are also relevant nowadays [14–17], since they can assist in optimizing the antenna structure and obtaining desirable characteristics. Therefore, combining the WG approach and the SA designing technology into one approach with a MoM core would be reasonable to take advantage of their benefits [18].

In [19], a MoM-WG core was used to modernize an approach to effectively model surface antennas. This approach was applied in modelling horn antennas. The obtained results were compared with the measured ones to verify the former, and the compared results showed good agreement. Based on the approach in [19], the researchers in [20] proposed another approach that can be used in modelling and manufacturing SAs. The authors called it “Optimal Current Grid Approximation” (OCGA). Using OCGA, an equivalent antenna structure in the form of a sparse grid can be obtained by excluding wires whose current magnitude is less than a specified level relative to the maximum. This level is referred to as the Grid Element Elimination Tolerance (GEET).

However, one limitation of using OCGA for non-printed antenna structures is the technical difficulties arising from the presence of free (unconnected) wires. To address this issue, a modified version of the original approximation, named “connecting” OCGA (COCGA), was proposed in [20]. COCGA preserves the physical connections of the grid wires and avoids breaking the main current paths in the antenna, thus reducing technical difficulties in manufacturing sparse antennas. In [21] the modelling and designing approaches are described in detail and verified on the example of only a horn and a conical horn antennas, but without any analysis of their efficiency regarding the change in GEET. These approaches are briefly summarized and presented here in this work for the integrity and clarity of the information. However, applying

this approach to typical antenna structures and verifying its results are necessary steps in developing this approach. It is also essential to estimate the performance of this approach regarding antenna characteristics, mass and cost reduction. Moreover, to determine the efficiency of this approach, it is crucial to assess its effectiveness in designing antennas in their sparse form or for subsequent modelling, instead of the original solid structures.

This study aims to evaluate the performance of the COCGA approach and verify its results by applying it to horn, conical horn, and reflector antennas and to summarize all the investigation done regarding developing these approaches. This will be achieved by considering three different types of antennas and with providing for the first time a comprehensive analysis of the obtained results regarding the change in GEET and with concluding general assessments of the approaches under study. This paper is organized as follows: Section II provide detailed explanations of the two approaches used in modelling and designing the antennas. Section III presents the results obtained by employing these approaches on three antenna structures, along with a comparative analysis of these results. Finally, Section IV summarizes the work done in this paper, presents the conclusions, and outlines the future work.

II. MODELLING AND DESIGNING APPROACHES

A. OCGA Brief Description

Applying the OCGA method in wire-grid antenna modelling allows for the reduction of mass, windage, and size while preserving the desired characteristics with controlled accuracy. To achieve this, the current vector elements obtained from the initial simulation are normalized based on the maximum current magnitude in the grid wires. Wires with a magnitude below a user-defined GEET coefficient are excluded from the grid. The resulting indexes of these wires are stored in a separate list, which is used to delete corresponding rows and columns from the system of linear algebraic equations (SLAE) matrix. The resulting impedance matrix is then used to construct a sparse antenna structure.

The obtained sparse structure can be utilized in subsequent antenna simulations, reducing computational costs. Additionally, if feasible, the sparse antenna can be manufactured in its final form. This results in a lighter and smaller antenna with acceptable characteristics compared to the original solid metal or wire-grid structure.

B. COCGA Brief Description

When implementing OCGA in antenna modelling, the resulting sparse structure may pose challenges for manufacturing, especially for non-printed antennas. Excluding certain wires can disrupt the physical connections and break the main current paths in the antenna. To address this, the OCGA algorithm can be modified to generate a more seamless sparse antenna structure that maintains these paths.

The modified approach involves constructing each section of the structure separately, with each section containing a group of connected wires aligned with their indexes in the

SLAE matrices. The wires are categorized as concentric (odd indexes) or radial (even indexes). After building all the sections to form the complete structure, OCGA is applied, resulting in a list of indexes corresponding to elements that need to be removed.

Before building the sparse structure, each element in the original list of wire indexes is checked to ensure that deleting the corresponding wire will not leave any wire without connections. The algorithm examines whether the wires that should be connected to the one under consideration are also marked for deletion. If so, the algorithm excludes the indexes of the first connected radial wire. The algorithm also verifies if this radial wire is connected to any concentric wire from its other end. If not, the algorithm proceeds to exclude further radial wires until a connection is established with a concentric wire or reaches a necessary level where all radial wires are connected. This level is determined based on the antenna's shape, and the wires at this level are crucial for forming the foundation of the physical structure.

As a result, a new list of indexes is obtained, containing wires that can be safely deleted without disrupting the current flow. Although the number of deleted wires is larger when applying COCGA compared to OCGA, the reduction in computational costs, mass, and size of the antenna varies slightly at the same GEET. Additionally, COCGA has the advantage of producing structures with more accurate characteristics compared to OCGA, as demonstrated in the following section. It can also help alleviate technical challenges in the manufacturing process.

III. RESULTS

To evaluate the performance of COCGA and verify its results, we applied it to horn [19], conical horn [22], and reflector [23] antennas. First, these antenna structures were modeled using the WG approach presented in [19]. Next, the OCGA and the COCGA were employed, and the results were compared with each other as well as with those of WG. Additionally, to verify their accuracy we compared the results obtained from COCGA with measured data or with those obtained using other numerical methods from other works.

A. Horn Antenna

First, we modeled a horn antenna using the approach outlined in [19]. The regular part of the antenna grid was divided into 8, 4, and 8 segments along the OX, OY, and OZ axes, respectively. The irregular part was divided into 16, 8, and 32 segments. The total number of wires (N) used to approximate the antenna surface was 3556. The antenna was excited by a wire with a 1 V potential difference, placed between the wide walls in the plane dividing the regular and irregular parts of the horn. Fig. 1a depicts the original WG structure of the antenna, while Fig. 2 showcases the normalized radiation patterns (RP) calculated and measured at 8 GHz [19]. The normalized field strength magnitudes were calculated in the E and H planes.

Next, we employed OCGA with a GEET value assumed to be 10%. Using the resulting SLAE, we constructed a sparse antenna structure with $N_S=2080$ wires, as shown in Fig. 1b.

The RPs of the sparse structure were compared with the calculated and measured patterns in Fig. 2. Solving the SLAE using Gaussian elimination consumes time proportional to $O(N)^3$, where N is the order of the SLAE, and the required memory is $O(N)^2$. Consequently, the antenna mass decreased by a factor of $N/N_s=1.71$, the required memory reduced by $(N/N_s)^2=2.92$, and the time for solving the SLAE decreased by $(N/N_s)^3=5$ times. Fig. 2 illustrates that the sidelobe level for the sparse structure is higher compared to the original one.

Subsequently, we applied COCGA, resulting in the sparse structure depicted in Fig. 1c. The calculated RPs in the E and H planes are compared with those obtained using OCGA and the measured patterns in Fig. 3. The resulting structure comprised 2168 wires. Thus, the antenna mass decreased by 1.64 times, the required memory by 2.69 times, and the time for solving the SLAE by 4.41 times. Although the reduction in computational cost and mass using COCGA is slightly less than with OCGA, the obtained sparse structure does not complicate the manufacturing process since there are no hanging wires. Moreover, the level of antenna RP sidelobes decreased significantly.

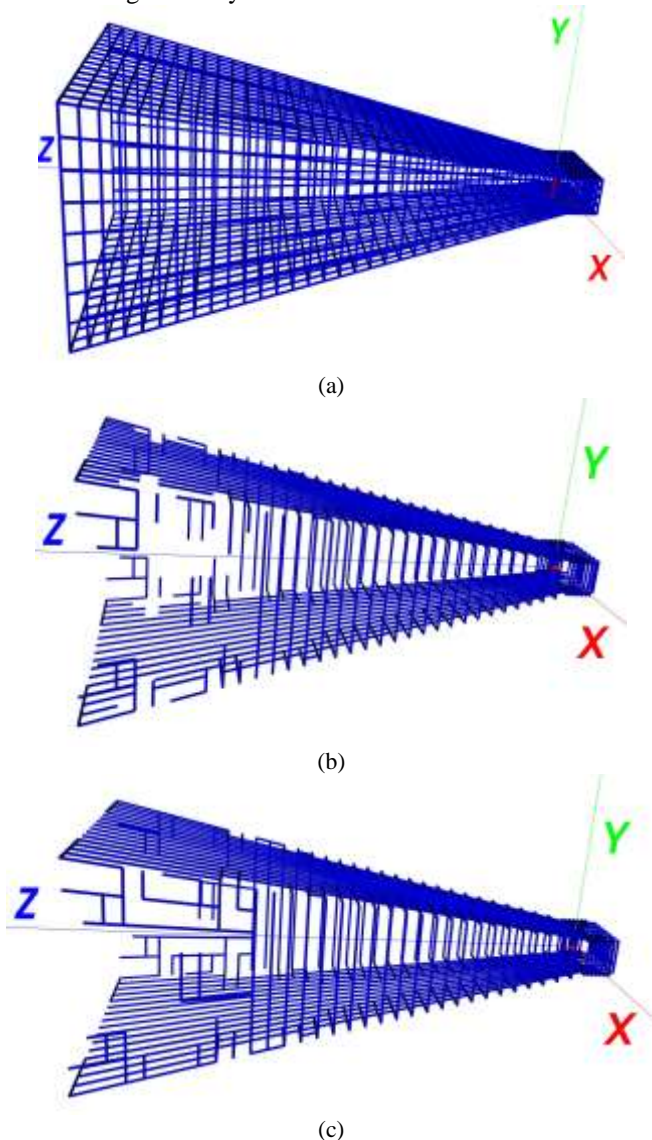


Fig. 1. Horn antenna structures: (a) original [19], (b) sparsified using OCGA and (c) COCGA

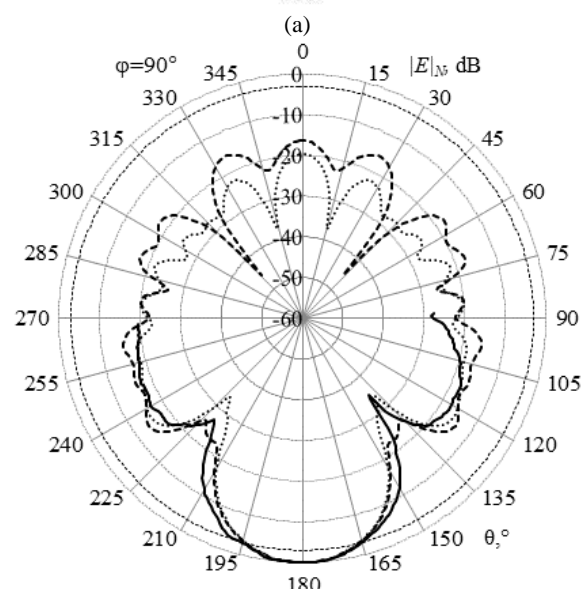
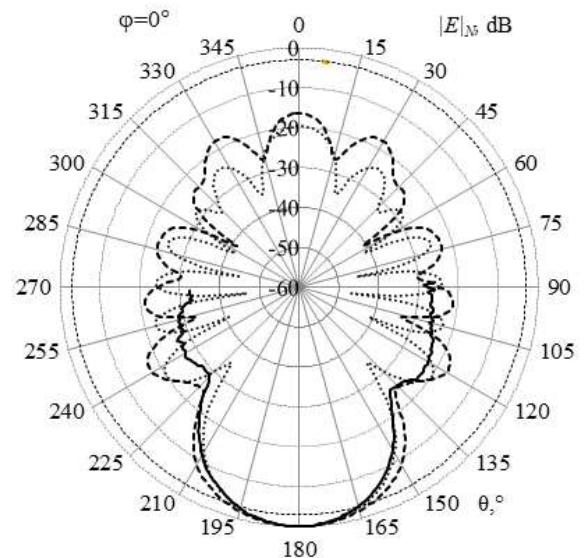
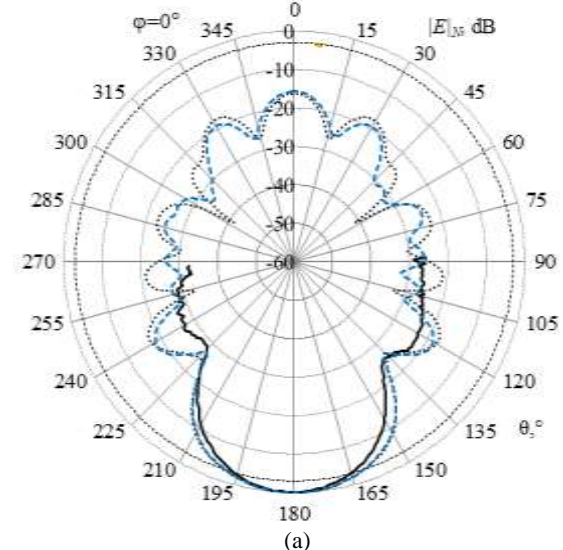


Fig. 2. Horn antenna RPs calculated for the original structure by WG [19] (···) and the structure sparsified by OCGA with GEET=10% (---) and the measured ones [19] (—) in:(a) the E and (b) H planes



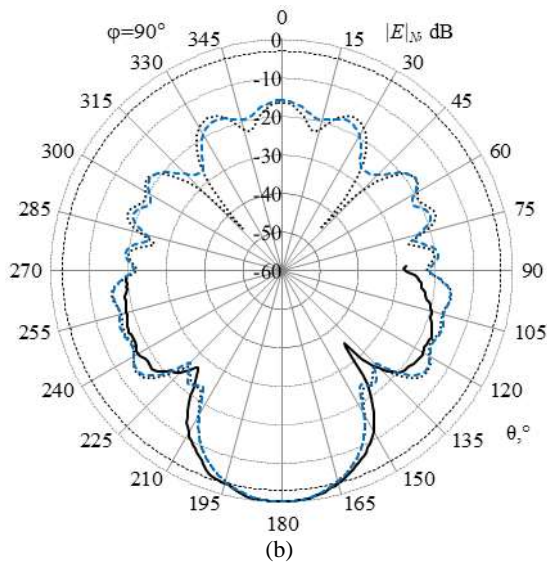


Fig. 3. Horn antenna RPs calculated by OCGA (···) and COCGA (---) with GEET=10%, and measured (—) ones in: (a) E and (b) H planes

B. Conical horn Antenna

In order to assess the effectiveness of COCGA on a conical horn antenna, we chose a specific antenna described in [22] and displayed in Fig. 4a. This antenna possesses distinct geometric parameters, including a 30 mm diameter for the regular part (d), a maximum diameter of 61.76 mm for the irregular part (D), a 31.25 mm height for the regular part (l_1), a 12 mm height for the irregular part (l_2), and a total horn height of 43.25 mm (L). To excite the antenna, a wire with a length of $l_d=0.36\lambda$ was positioned at the center of the intersection between the regular and irregular parts. Initially, we modelled the antenna using the WG approach outlined in [19], where all grid wires were assigned a radius of 0.1 mm. The approximation of the antenna surface required a total of 3600 wires (N), as depicted in Fig. 4b, referred to as the original structure. The resulting RPs of the original conical horn antenna structure, obtained through WG approximation, were then compared to those derived using the finite difference time domain (FDTD) method [22] at an 8 GHz frequency. The comparison of antenna gains (AG) was carried out in the E and H planes, displaying favorable agreement (Fig. 5). Notably, the modelling process using the WG approach [19] was completed in 29.92 seconds, exhibiting a 1.34 times faster performance than the FDTD method [22] while utilizing the same computational resources.

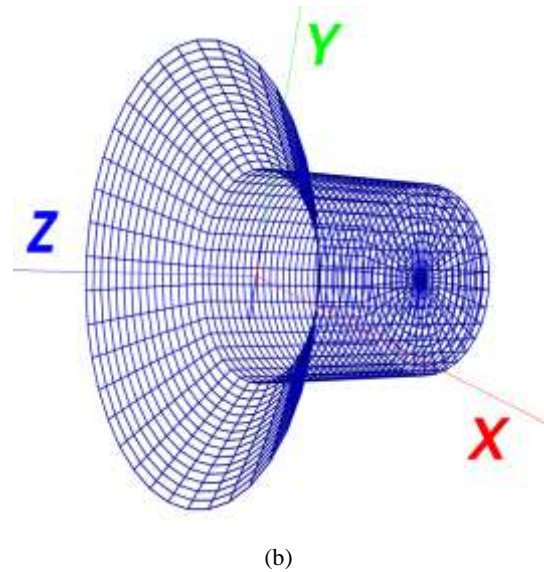
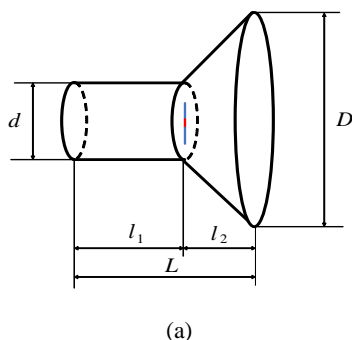


Fig. 4. (a) Conical horn antenna isometric view [22] and (b) the structure of the antenna approximated using the WG approach [19]

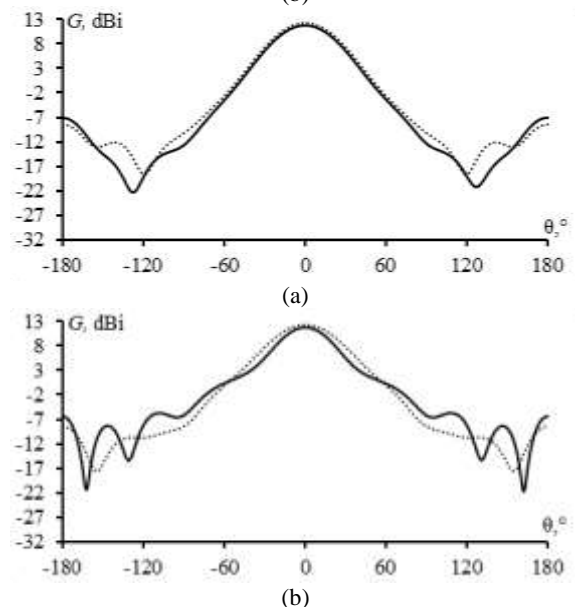


Fig. 5. Conical horn AGs calculated for the original structure (···) obtained by WG [19] and those calculated by FDTD [22] (—) in the: (a) E plane and (b) H plane

Next, we applied OCGA to obtain sparse antenna RPs with GEET value of 6% and 10%. The resulting sparse antennas are shown in Fig. 6, with $N_S=2846$ wires in the grid at 6%, and $N_S=2362$ wires at 10%. We then compared the obtained RPs in the E and H planes with those obtained using FDTD in [22] (Fig. 7). As seen, with increasing GEET value, the divergence of the results increases, but the radiation in the main direction remains acceptable. OCGA application results in a reduction in the antenna mass by 1.26 times at GEET of 6% and by 1.52 times at 10%. The reduction in required memory was 1.60 and 2.32 times at GEET of 6% and 10%, respectively, and in the required time for solving SLAE was 2.02 and 3.54 times, at GEET of 6% and 10%, respectively. The total time spent on the simulation by OCGA at GEET of 6% and 10% was 18.42 s and 12.92 s, respectively, which was 2.17 and 3.09 times faster than that spent by FDTD [22].

Using COCGA, we obtained sparse antennas with GEET values of 6% and 10% (Fig. 8), consisting of 2850 and 2442 wires in their grids, respectively. The RPs of the resulting antennas were compared with those obtained using FDTD [22] in the *E* and *H* planes (Fig. 9). As a result of employing COCGA, the mass of the antenna decreased by 1.26 and 1.47 times, the required memory by 1.60 and 2.17 times, and required time by 2.02 and 3.20 times at GEET values of 6% and 10%, respectively. The time spent on simulation using COCGA at GEET values of 6% and 10% was 18.69 s and 14.08 s, which is 2.14 and 2.84 times faster than using FDTD [22].

To compare the results obtained with OCGA and COCGA, we present them in Fig. 10. It is evident that the results obtained with COCGA have less divergence from those obtained using FDTD than those obtained with OCGA as the GEET value increases. In addition, the results after OCGA and COCGA at GEET=6% are identical, while at 10% they differ, and the divergence is well noticed in the sidelobes. Nevertheless, the results in the main direction have a good agreement. This again proves the advantage of using COCGA over OCGA in terms of modelling accuracy and ease of manufacturing.

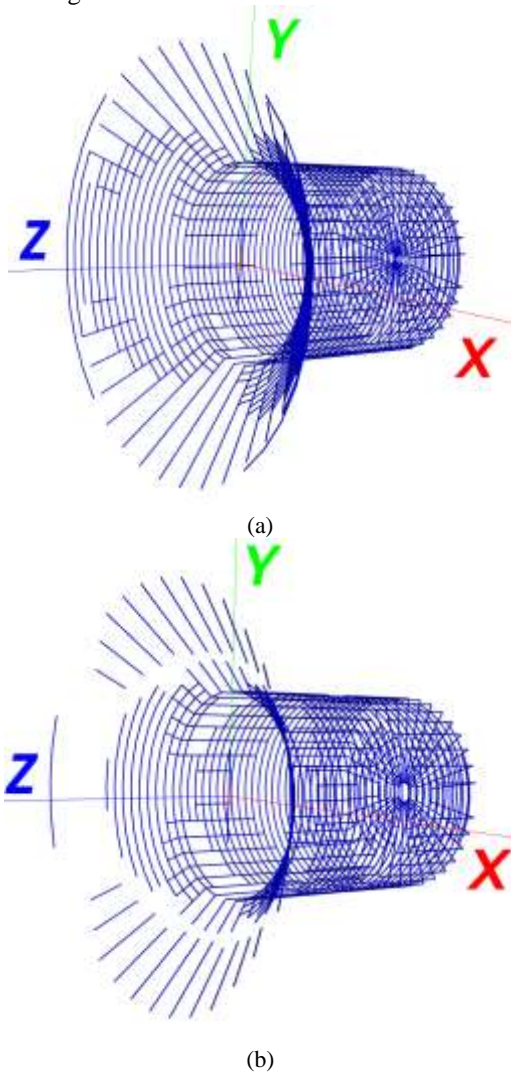


Fig. 6. Sparse antenna structures obtained using OCGA with GEET: (a) 6% and (b) 10%

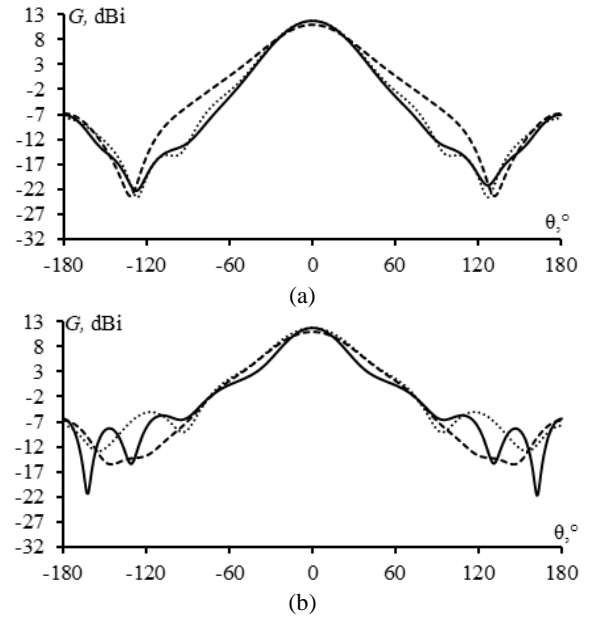


Fig. 7. Conical horn AGs calculated for structure obtained using OCGA with GEET of 6% (···) and 10% (---) and those calculated using FDTD [22] (—) in the: (a) *E* plane and (b) *H* plane

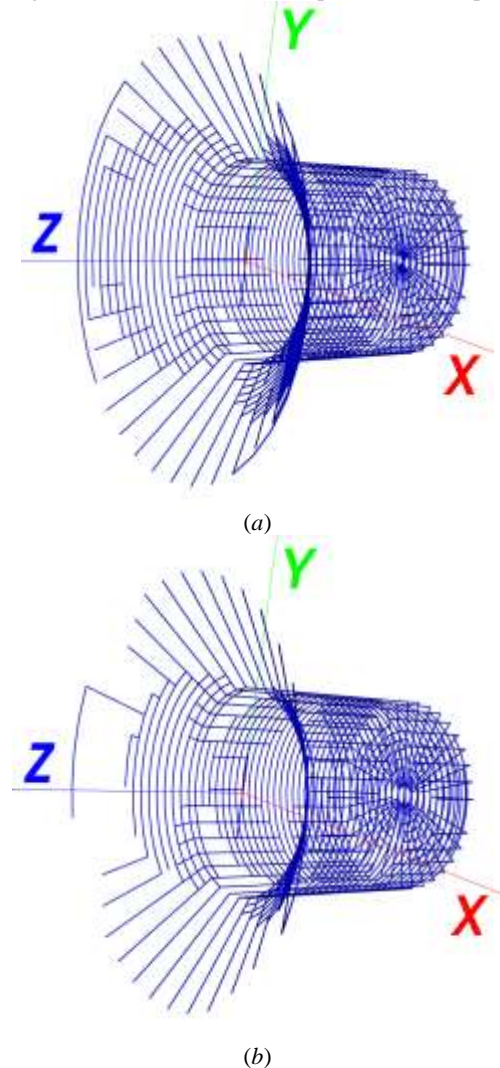


Fig. 8. Sparse antenna structures obtained using COCGA with GEET: (a) 6% and (b) 10%

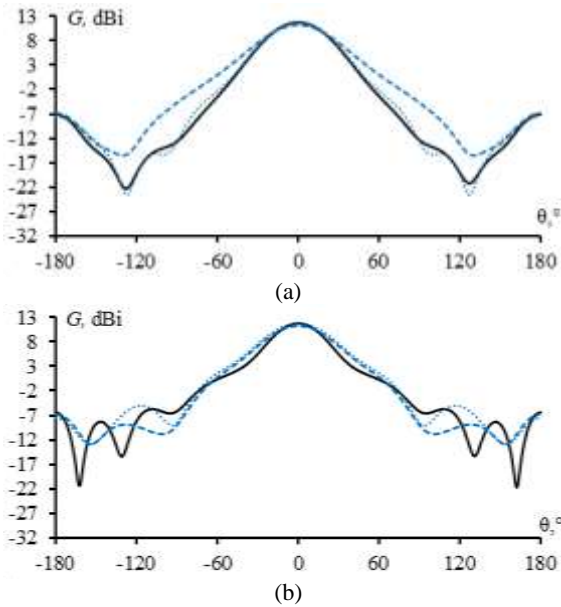


Fig. 9. Conical horn AGs calculated for structure obtained using COCGA with GEET of 6% (···) and 10% (---) and those calculated using FDTD [22] (—) in the: (a) E plane and (b) H plane

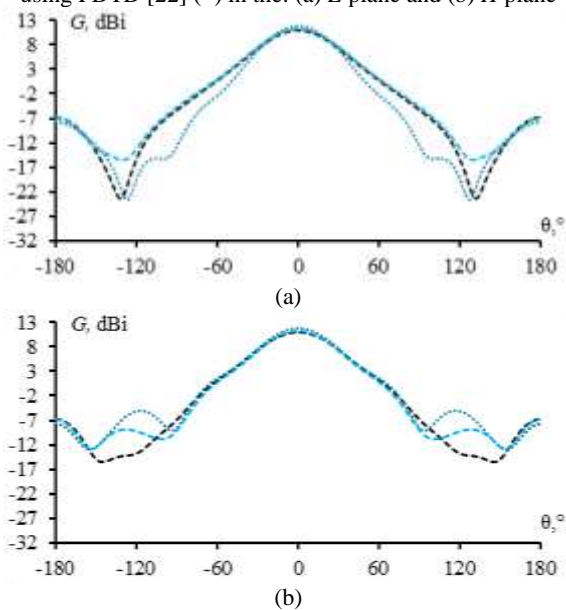


Fig. 10. Conical horn AGs for structures obtained using OCGA with GEET of 6% (···) and 10% (---) and those obtained using COCGA with GEET of 6% (···) and 10% (---) in the: (a) E plane and (b) H plane

C. Reflector Antenna

To verify effectiveness of COCGA on a reflector antenna, we chose the antenna produced in [23]. The isometric view of the antenna structure is presented in Fig. 11a, and it has the following geometrical parameters: diameter $D=400$ mm, depth $h=143.6$ mm, and focus $F=75$ mm. To excite the antenna, we used a wire with a length of $l=\lambda/3.6$ and a radius $R_1=\lambda/3.6$, placed at a distance equal to the focus of the reflector from the center of the grid. When modelling using the approaches from [19], we divided the WG of the reflector antenna into 60 radial and 25 concentric parts. The total number of wires (N) with a radius $R_2=\lambda/30$ used to approximate the antenna surface

was 3000. Fig. 11b shows the structure of the antenna approximated using WG (hereinafter referred to as the original structure). We compared the obtained antenna RPs for the original structure with the measured results in [23]. The AG was calculated at the frequencies of 5.1 GHz and 5.9 GHz in the E (Fig. 12) and H (Fig. 13) planes, and compared to the measured ones.

Subsequently, we applied OCGA with a GEET value of 10% to generate the sparse antenna radiation patterns at frequencies of 5.1 GHz and 5.9 GHz. The resulting sparse antennas are illustrated in Fig. 14, with $N_s=1988$ wires at 5.1 GHz and 2112 wires at 5.9 GHz. The application of OCGA led to a reduction in antenna mass by 1.51 times at 5.1 GHz and 1.42 times at 5.9 GHz. Additionally, the required memory decreased by 2.28 and 2.02 times, respectively, and the solution time for SLAE decreased by 3.44 and 2.88 times at 5.1 GHz and 5.9 GHz, respectively. Moving forward, we employed COCGA to obtain sparse antennas with a GEET value of 10% at frequencies of 5.1 GHz and 5.9 GHz (Fig. 15). The number of wires in their grids amounted to 2027 at 5.1 GHz and 2166 at 5.9 GHz. By utilizing COCGA, the antenna mass decreased by 1.48 and 1.39 times, the required memory decreased by 2.19 and 1.92 times, and the solution time decreased by 3.25 and 2.66 times at 5.1 GHz and 5.9 GHz, respectively.

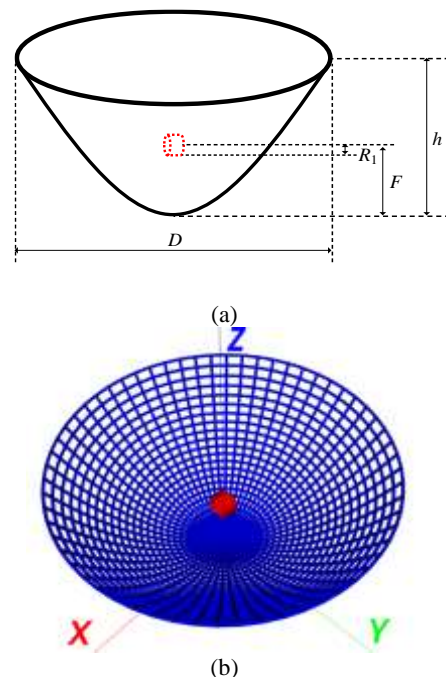
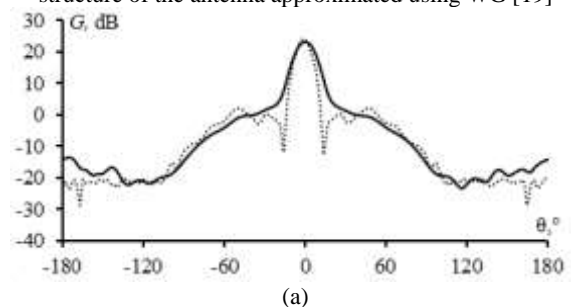


Fig. 11. (a) Isometric view of the reflector antenna [23] and (b) the structure of the antenna approximated using WG [19]



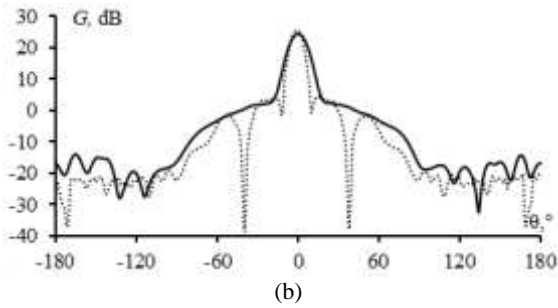


Fig. 12. Reflector AGs obtained using the WG (—) compared to those measured in [23] (···) in the *E*-plane at: (a) 5.1 and (b) at 5.9 GHz

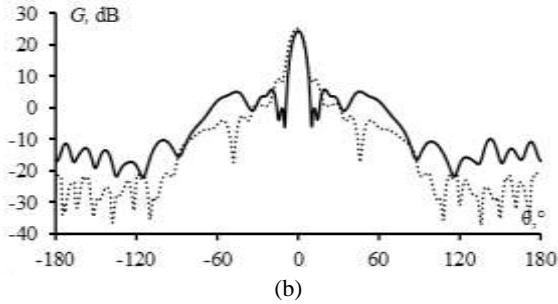
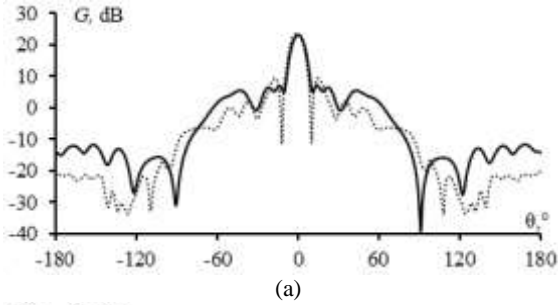


Fig. 13. Reflector AGs obtained using the WG (—) compared to those measured in [23] (···) in the *H*-plane at: (a) 5.1 and (b) 5.9 GHz

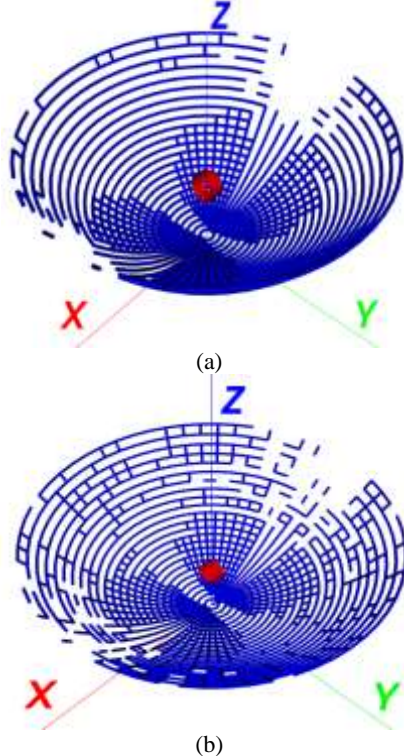


Fig. 14. Sparse reflector antenna structures obtained using OCGA at: (a) 5.1 and (b) 5.9 GHz

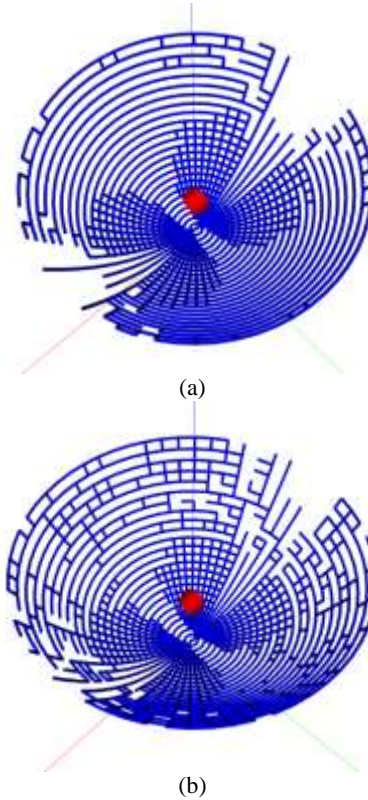
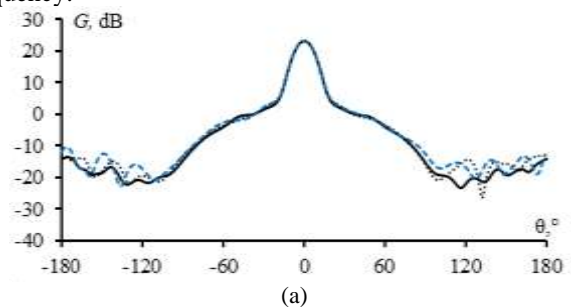


Fig. 15. Sparse reflector antenna structures obtained using COCGA at: (a) 5.1 and (b) 5.9 GHz

The comparison of AGs at 5.1 GHz and 5.9 GHz, calculated using the WG approach (original structure), OCGA (sparse structure), and COCGA (sparse structure), are presented in Fig. 16 for the *E*-plane and Fig. 17 for the *H*-plane. The results obtained using the sparse antennas align closely with the measured values and those obtained using the WG approach. Notably, there is a larger discrepancy in the results at 5.1 GHz, while at 5.9 GHz, the sparse antennas obtained with COCGA exhibit lower levels of sidelobes and zero radiation points compared to those obtained with OCGA (on average by 10 dB).

To demonstrate the feasibility of using sparse antennas obtained by the COCGA method, we took the sparse antenna generated at a frequency of 5.9 GHz and modelled it at a frequency of 5.1 GHz. Subsequently, we compared the resulting characteristics and presented them in Fig. 18. As shown, the COCGA method effectively generates sparse antennas that can operate in a range of frequencies without significantly altering their characteristics, despite the fact that the surface current flows in different directions at each frequency.



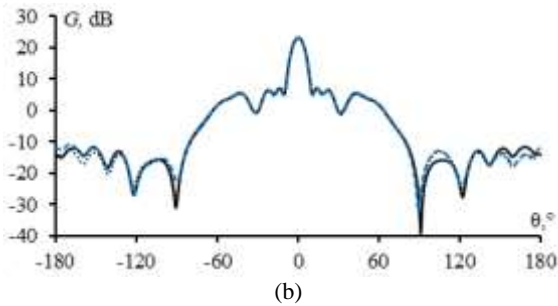


Fig. 16. Reflector AGs of the original structure (—) compared to those of the sparse structures obtained using OCGA (···) and COCGA (---) in the E -plane at: (a) 5.1 GHz and (b) 5.9 GHz

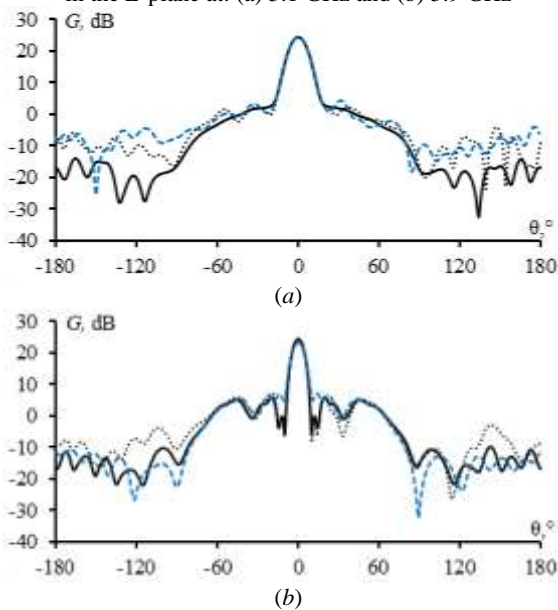


Fig. 17. Reflector AGs of the original structure (—) compared to those of the sparse structures obtained using OCGA (···) and COCGA (---) in the H -plane at: (a) 5.1 GHz and (b) 5.9 GHz

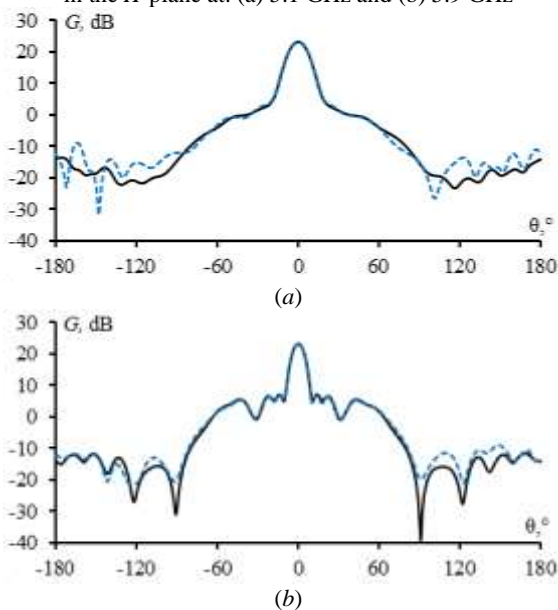


Fig. 18. Reflector AGs calculated at 5.1 GHz for the antenna sparsed by the COCGA (---) from the WG structure at 5.9 GHz compared to that obtained using the WG (—) (original structure) at 5.1 GHz in the: (a) E -plane and (b) H -plane with GEET=10%

D. Comparative Analysis: GEET Dependences

When creating sparse antenna structures and after increasing the GEET value according to the manufacturer's needs, a significant number of wires will be discarded. This, in turn, will cause a change in the antenna characteristics. However, for each antenna type, the change will be different depending on the GEET value. Therefore, a more general comparison of the properties of each antenna after applying OCGA and COCGA to the WG antenna is necessary to have an overview. This will assist designers in selecting the GEET value that best suits their requirements.

E. Horn Antenna

For the horn antenna, Fig. 19 shows the change in the number of wires after altering the GEET value. It is evident that the number of remaining conductors in the sparse antenna structure is consistently higher after COCGA compared to OCGA. This can be attributed to the restoration of some wires to maintain the antenna's seamless structure.

The total number of remaining wires in a sparse antenna can significantly affect its characteristics and mass. As shown in Fig. 19, there is not much difference in the total number of wires when the GEET value is less than 10% for both OCGA and COCGA methods. The results also indicate that the characteristics of the original WG antenna and the sparse one are nearly identical when the GEET value is less than 10%. However, when the GEET value exceeds 10%, the sparse antenna obtained using OCGA shows a sharp reduction in AG and differs greatly from the original WG antenna element (Fig. 19). On the other hand, COCGA produces a slower change that results in characteristics closer to those of the original WG antenna ones. Additionally, the reductions in the antenna mass and in the time and memory required to simulate it change linearly when the GEET value changes, as depicted in Fig. 20. Other antenna characteristics are also compared and presented in Table 1.

TABLE 1
THE HORN ANTENNA CHARACTERISTICS FOR THE APPROXIMATION APPROACHES COMPARED TO THOSE FOR THE ORIGINAL WG STRUCTURE AND MEASURED ONES

Antenna model	f, GHz	G_{\max} , dBi	Sidelobes level (E/H), dB	BW (E/H), °
Measured	8	—	22.35/17.43	32/32
WG	8	23.73	19.96/15.54	32/28
OCGA	8	23.77	17.26/13.96	38/28
COCGA	8	22.79	19.18/14.89	36/28

The obtained results show that, for the horn antenna, OCGA outperforms COCGA in terms of mass and resource reduction when GEET is greater than 10%. However, it provides less accuracy than the results obtained with COCGA. This can be easily explained because COCGA creates a seamless structure and does not interrupt the path of the current.

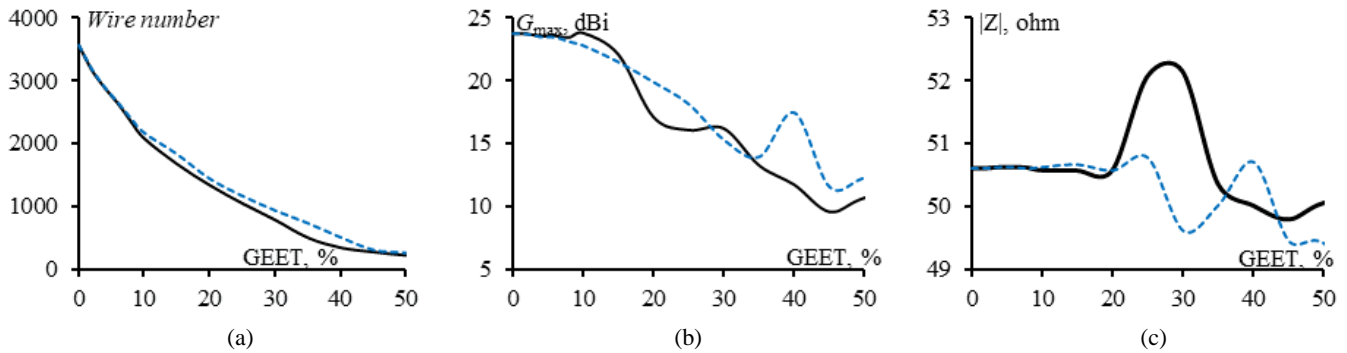


Fig. 19. Sparse WG horn antenna structure against GEET after applying OCGA (–), and COCGA (---): (a) total remains wires number, (b) its maximum gain, and (c) its input impedance magnitude

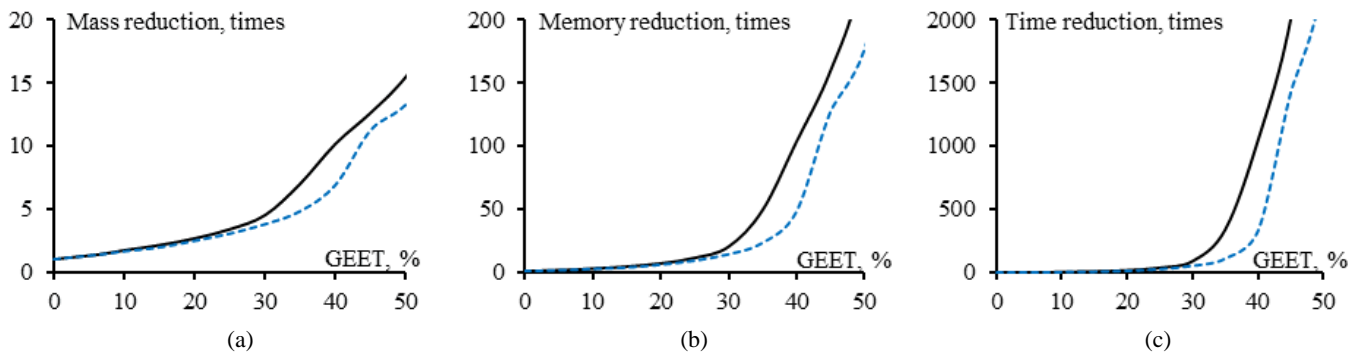


Fig. 20. Sparse WG horn antenna against GEET value after OCGA (–) and COCGA (---): (a) mass reduction, (b) the memory and (c) time reduction on further simulation

Therefore, it is recommended to use OCGA when it is necessary to reduce the computational cost of modelling, especially in the case of investigating the antenna properties where a rapid estimation without strict requirements is required. On the other hand, when high accuracy of results is required, using COCGA is the most appropriate option, as it can greatly reduce the weight while providing results closest to those of the original antenna.

F. Conical Horn Antenna

Similarly, the change of the remaining wires for the conical horn antenna and its maximum AGs and input impedance with changing the GEET value are shown in Fig. 21. In addition, the relationship between GEET and the mass, memory and calculation time reduction are shown in Fig. 22.

It can be observed that the conclusions drawn for the conical horn antenna are not significantly different from those made for the horn antenna. However, as the GEET value is increased, the variation in AG value is not as linear as observed in the horn antenna, particularly after OCGA. This can be helpful in finding a high GEET value, which results in a significant reduction in mass and computational cost while still maintaining acceptable antenna characteristics. Table 2 compares the characteristics of sparse WG antennas at various GEET values with those of the original WG structure and those obtained using the FDTD method. From Table II it can be seen that the results obtained after OCGA and COCGA do not considerably differ. But in general, the COCGA results are

closer to the results obtained by WG and FDTD at the same GEET value.

TABLE 2

THE CONICAL HORN ANTENNA CHARACTERISTICS FOR THE APPROXIMATION APPROACHES COMPARED TO THOSE FOR THE ORIGINAL STRUCTURE AND TO THOSE OBTAINED USING FDTD

AE model	G _{max} , dBi	VSWR	Sidelobe level (E/H), dB	BW (E/H), °
FDTD [22]	11.9	1.14	18.91/18.28	44/38
WG	12.24	1.80	20.70/20.70	46/48
OCGA (6%)	11.68	1.77	19.47/19.47	46/50
OCGA (10%)	11.08	1.80	17.77/17.81	52/54
COCGA (6%)	11.68	1.79	19.28/19.28	46/50
COCGA (10%)	11.12	1.77	18.01/18.01	52/50

G. Reflector Antenna

The GEET dependencies of the total number of remaining wires after employing OCGA and COCGA on the reflector antenna WG structure are presented in Fig. 23a. The changes in AGs and input impedance are demonstrated in Fig. 23b, c as the GEET value is changed. The reduction in antenna mass, memory, and simulation time with changing GEET value is shown in Fig. 24. Using the approximations under study on a WG antenna structure produces a sparse structure with almost no characteristic difference between them when GEET value is up to 15%. Beyond 15%, the difference becomes more

obvious. In addition, despite the COCGA disadvantages, it leads to sparse antenna structures that can be easily manufactured with acceptable accuracy of its characteristics.

TABLE 3

THE REFLECTOR ANTENNA CHARACTERISTICS FOR THE APPROXIMATION APPROACHES COMPARED TO THOSE FOR THE ORIGINAL WG STRUCTURE AND MEASURED ONES

AE model	f, GHz	G_{\max} , dBi	VSWR	Sidelobe level (E/H), dB	BW (E/H), °
Measured [23]	5.1	24.5±1	≤1.5	21.96/14.04	≈9
	5.9			22.23/23.72	
WG	5.1	23.27	1.22	23.27/17.56	12/8
	5.9	24.49	1.25	24.49/18.69	12/8
OCGA	5.1	23.15	1.22	23.03/15.99	12/8
	5.9	24.22	1.26	21.68/19.02	12/8
COCGA	5.1	23.17	1.22	23.15/16.20	12/8

This is also confirmed by the data in Table 3 where the AG, VSWR, sidelobe level, and maximum beam width at -3 dB are calculated for the sparse antenna structures obtained after employing OCGA and COCGA and compared with the measured results from [23].

IV. CONCLUSION

The OCGA and COCGA approaches that can be used for modelling and designing sparse wire-grid antenna structures have been investigated and verified in this work. They were

employed to three antenna structures. The results obtained using these approaches are compared with those obtained using other numerical methods or measurements results from other works. The presented results were also compared between each other to estimate their efficiency. In particular, it was shown that COCGA can be perfectly generate antenna structures that can be used in manufacturing antennas since it preserves the structure integrity. Moreover, the structures generated by COCGA can be used as an equivalent model of the original solid antenna structure in the antenna modelling process. This is explained by the fact that this model requires less computational resources for further simulations with maintaining an acceptable level of the results accuracy.

Further research can be directed toward investigating the adaptability, performance, and possibility of applying these approaches for different types of antennas, including printed antennas and antenna structures with the presence of a dielectric in general. Furthermore, it should be noted that these approaches can indeed be used as the core of an optimization procedure to obtain sparse antennas with certain required characteristics and controlled accuracy, which is the next prior step in improving the sparse antenna design process, and to formulate and summarize all the usage aspects of these approaches, their capabilities, advantages and disadvantages.

ACKNOWLEDGEMENT

This research was funded by the Ministry of Science and Higher Education of the Russian Federation project FEWM-2023-0014.

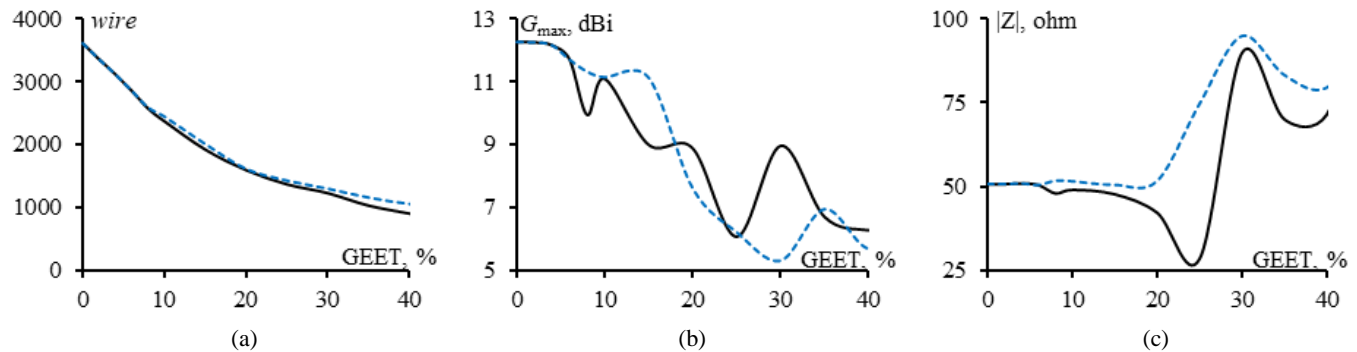


Fig. 21. Sparse WG conical horn antenna structure against GEET value after OCGA (—) and COCGA (---): (a) total remains wires number, (b) its maximum gain, and (c) its input impedance magnitude

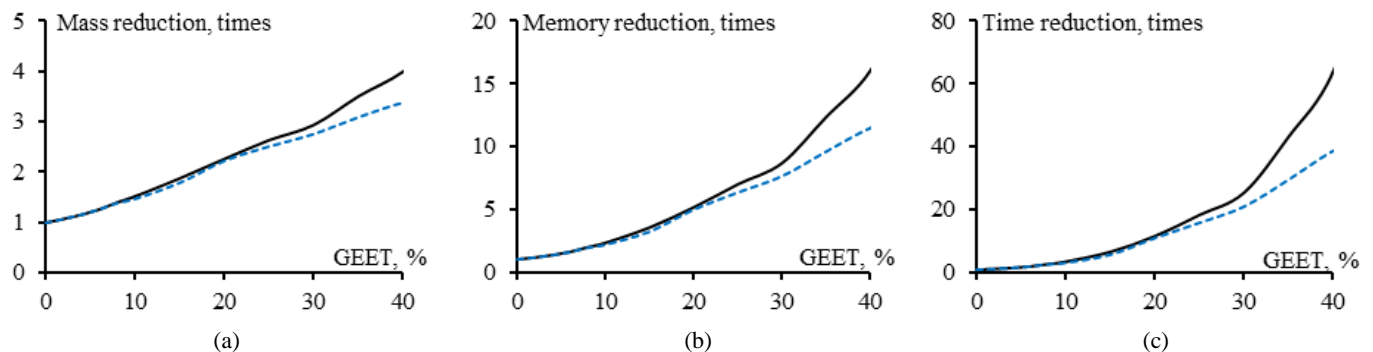


Fig. 22. Sparse WG conical horn antenna against GEET value after OCGA (—) and COCGA (---): (a) mass reduction, (b) the memory and (c) time reduction on further simulation

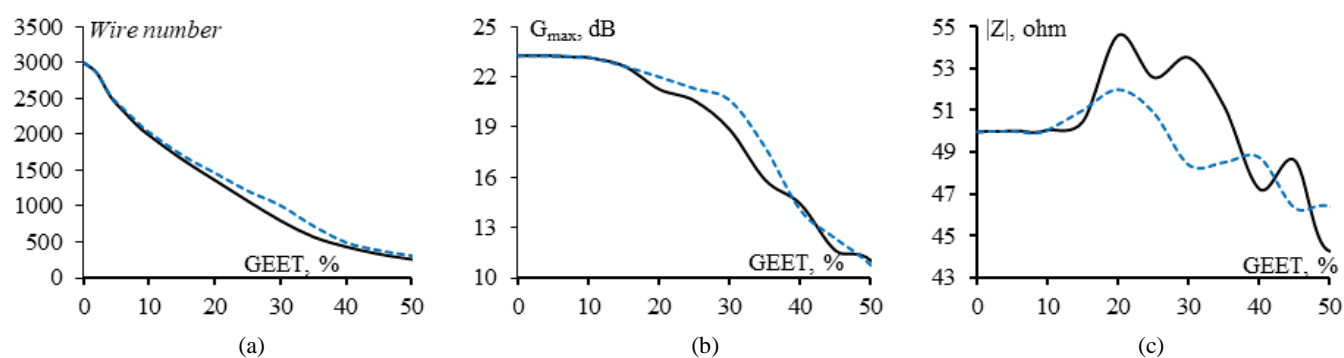


Fig. 23. Sparse WG reflector antenna structure against GEET value after OCGA (—) and COCGA (---): (a) total remains wires number, (b) its maximum gain and (c) its input impedance magnitude

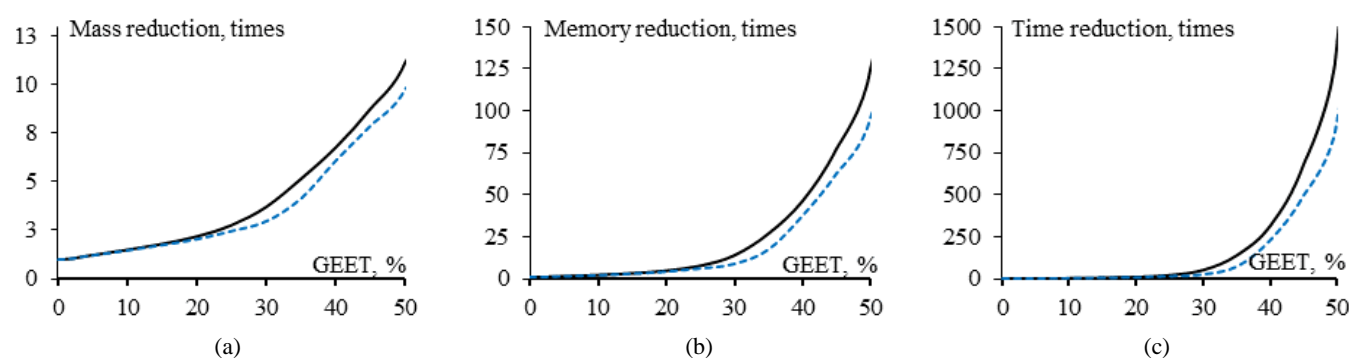


Fig. 24. Sparse WG reflector antenna against GEET value changing from 0% to 50% after OCGA (—) and COCGA (---): (a) mass reduction (b) the memory and (c) time reduction on further simulation

REFERENCES

- [1] O.P. Kumar, P. Kumar, T. Ali, P. Kumar and S. Vincent, "Ultrawideband Antennas: Growth and Evolution", *Micromachines*, vol. 13, no. 1, p. 60, Dec. 2021.
- [2] A. Jabbar, Q.H. Abbasi, N. Anjum, T. Kalsoom, N. Ramzan, S. Ahmed, P.M. Rafi-ul-Shan, O.P. Falade, M.A. Imran and M. UrRehman, "Millimeter-Wave Smart Antenna Solutions for URLLC in Industry 4.0 and Beyond", *Sensors*, vol. 22, no. 7, p. 2688, Mar. 2022.
- [3] J.L. Gómez-Tornero, "Smart Leaky-Wave Antennas for Iridescent IoT Wireless Networks", *Antenna and Array Technologies for Future Wireless Ecosystems, IEEE*, pp. 119-181, 2022.
- [4] U. Ali, S. Ullah, B. Kamal, L. Matekovits and A. Altaf, "Design, Analysis and Applications of Wearable Antennas: A Review", *IEEE Access*, vol. 11, pp. 14458-14486, 2023.
- [5] S. Noghianian and S.K. Sharma, "Radiation Pattern Reconfigurable Antennas", *Multifunctional Antennas and Arrays for Wireless Communication Systems, IEEE*, pp. 67-121, 2021.
- [6] I. Munina, I. Grigoriev, G. O'donnell and D. Trimble, "A Review of 3D Printed Gradient Refractive Index Lens Antennas", *IEEE Access*, vol. 11, pp. 8790-8809, 2023.
- [7] G. Amendola et al., "Low-Earth Orbit User Segment in the Ku and Ka-Band: An Overview of Antennas and RF Front-End Technologies", *IEEE Microwave Magazine*, vol. 24, no. 2, pp. 32-48, 2023.
- [8] M. Liang, C. Shemelya, E. MacDonald, R. Wicker and H. Xin, "3-D Printed Microwave Patch Antenna via Fused Deposition Method and Ultrasonic Wire Mesh Embedding Technique", *IEEE Antennas and Wireless Propagation Letters*, vol. 14, pp. 1346-1349, 2015.
- [9] R.F. Harrington, "Matrix methods for field problems", *Proceedings of the IEEE*, vol. 55, no. 2, pp. 136-149, Feb. 1967.
- [10] S. Rao, "A Simple and Efficient Method of Moments Solution Procedure for Solving Time-Domain Integral Equation—Application to Wire-Grid Model of Perfect Conducting Objects", *IEEE Journal on Multiscale and Multiphysics Computational Techniques*, vol. 4, pp. 57-63, 2019.
- [11] S.N. Makarov, *Antenna and EM Modeling with MATLAB*. New York, NY, USA: John Wiley & Sons, 2002.
- [12] X. Zhu, W. Wu, G. Zhang and L. Cai, "Analysis of Radiation Field of a New Wire-grid TEM Horn", *Photonics & Electromagnetics Research Symposium-Fall (PIERS-Fall)*, pp. 3188-3191, Xiamen, China, 2019.
- [13] J.L. Kubwimana and N. Kirsch, "The Impedance of Optically Transparent Thin Mesh Wire RF Devices", *Photonics & Electromagnetics Research Symposium (PIERS)*, pp. 85-91, Hangzhou, China, 2021.
- [14] D. Silverstein and Y. Leviatan, "Design of Irregular Embedded Antenna Arrays for Shaped-Beam Radiation Using Reciprocity and Sparse Optimization", *IEEE Transactions on Antennas and Propagation*, vol. 71, no. 4, pp. 3273-3281, 2023.
- [15] S.R. Shebert, M.G. Amin, B.H. Kirk and R.M. Buehrer, "Multi-Signal Classification Using Deep Learning and Sparse Arrays", *IEEE Military Communications Conference (MILCOM)*, pp. 1-6, Rockville, MD, USA, 2022.
- [16] Q. Liu, K. Cao, Y. Cheng and H. Wang, "Sparse Array Radar Staring Imaging Based on Matrix Completion", *International Conference on Microwave and Millimeter Wave Technology (ICMMT)*, pp. 1-3, Harbin, China, 2022.
- [17] V.V. Golovin and Y.N. Tyschuk, "Investigation of the Characteristics of A Deployable Space Mirror Antenna with A

- Sparse Reflecting Surface”, *Journal of Radio Electronic*, no. 1, 2023. (in Russian)
- [18] V.V. Yatsenko, S.A. Tretyakov, S.I. Maslovski and A.A. Sochava, “Higher Order Impedance Boundary Conditions for Sparse Wire Grids”, *IEEE Transactions on Antennas and Propagation*, vol. 48, no. 5, pp. 720-727, 2000.
- [19] A. Alhaj Hasan, D.V. Klyukin, A.A. Kvasnikov, M.E. Komnatnov and S.P. Kuksenko, “On Wire-Grid Representation for Modeling Symmetrical Antenna Elements”, *Symmetry*, vol. 14, no. 7, p. 1354, 2022.
- [20] A. Alhaj Hasan, T.M. Nguyen, S.P. Kuksenko and T.R. Gazizov, “Wire-Grid and Sparse Mom Antennas: Past Evolution, Present Implementation And Future Possibilities”, *Symmetry*, vol. 15, no. 2, p. 378, 2023.
- [21] A.A. Hasan, T.M. Nguyen and T.R. Gazizov, “Wire Grid Sparse Antennas: Verification of a Modified Modeling Approach”, *2023 IEEE Ural-Siberian Conference on Biomedical Engineering, Radioelectronics and Information Technology (USBREIT)*, pp. 100-104, Yekaterinburg, Russian Federation, 2023.
- [22] F. Shamshad and M. Amin, “Simulation Comparison between HFSS and CST for Design of Conical Horn Antenna”, *Journal of Expert Systems (JES)*, vol. 1, no. 4, p. 84-90, 2012.
- [23] *Jirous antennas direction for your waves*. Available online: https://en.jirous.com/antenna-5ghz-parabolic/jrc-24DD_MIMO (accessed on June 10, 2023).